A novel two-stage gasification strategy for nitrogen-free syngas production- pilot-scale experiments

Tchini Séverin Tanoh, Amina Ait Oumeziane, Jérôme Lemonon, Francisco Javier Escudero Sanz, Sylvain Salvador

A novel two-stage gasification strategy for nitrogen-free syngas production-pilot-scale experiments

Tchini Séverin Tanoh *, Amina Ait Oumeziane, Jérôme Lemonon, Francisco Javier Escudero-Sanz, Sylvain Salvador

Université de Toulouse, IMT Mines Albi, UMR CNRS 5302, Centre RAPSODEE, Campus Jarlard, F-81013 Albi Cedex 09, France

Keywords:
Green waste
Pyrolysis
Non-catalytic reforming
Rotary kiln
Tubular reactor
Soot

A B S T R A C T

Green waste and wood gasification have been studied through a non-catalytic process. Experiments are conducted at a pilot-scale developed at RAPSODEE Centre to validate the feasibility of producing high-quality nitrogen-free syngas. Biomass is first pyrolyzed at 800 °C in a rotary kiln. Then, the volatile matter is cracked and reformed in a non-catalytic tubular reactor. Effects of temperature and gas residence time in the tubular reactor on the process performances are evaluated. The results show that the tar formed in the first stage for each biomass is mainly converted into soot inside the second one. The soot yield has reached 11.5 wt% at 1300 °C with a gas residence time of 10 s. Wood tar appears to have a different suite of compounds than tar from green waste; they probably have different cracking pathways. The wood tar conversion ratio has achieved 98.8% at 1300 °C with a gas residence of 5 s while it reaches only 80.4% for green waste. Under these operating conditions, the lower heating value of syngas is around 11 MJ/Nm^3. The syngas obtained is rich in H_2 (up to 50 vol %) and CO (up to 35 vol%) and contains CO_2 (<10 vol%) and CH_4 (< 5 vol%).

1. Introduction

Setting reliable strategies to replace fossil energies with renewable and sustainable ones is one of the biggest and urgent challenges of our era. Indeed, to make up for the environmental impact due to the increase of world energy consumption, innovative and efficient solutions are required. Because of its carbon neutrality, energy recovery from biomass is one of the most promising alternatives [1]. France has adopted "the Energy Transition for Green growth Act -LTECV" to increase renewable gas (biomethane) consumption up to 10% by 2030 to reduce the impact of natural gas consumption on the environment. For that purpose, various technologies such as anaerobic digestion, pyrolysis and gasification followed by methanation are used to produce renewable gas from biomass [2].

Large amounts of very dispersed biomass are constantly generated. They may come from gardens, industrial processes, agricultural activities etc. Non-lignocellulosic biomass can be, for example, transformed into biogas containing 50 to 70% of methane by anaerobic digestion. Then, it is purified to achieve the same quality as natural gas and injected into distribution networks. According to France's Ministry of Environmental and Solidarity-based Transition, 35 sites of biogas produced by anaerobic digestion are injecting biomethane into the gas network, supplying the equivalent of 315 GWh of annual production or 0.05% of France's total gas consumption. Hence, anaerobic digestion alone is not able to cover all the country's needs. Indeed, the majority of the produced biomass is lignocellulosic. Due to its physical and chemical properties, lignocellulosic biomass cannot undergo biodegradation without extensive pre-treatment [3].

Another alternative to biomass biodegradation can be the use of thermochemical processes such as pyrolysis and gasification, to produce syngas (CO, CO_2, and H_2) from lignocellulosic biomass, which can be subsequently converted to methane by methanation. This research work is focused on the production of syngas for biological methanation.

Various gasification techniques can be used to produce syngas from biomass [4,5]. One major difficulty when using a thermochemical pathway to produce a syngas destined for methanation is tar removal [6,7]. For this purpose, researchers have developed processes to produce a tar-free syngas. Such processes consist mainly of two reactors, the first dedicated to biomass pyrolysis and the second to thermal cracking and reforming of pyrolysis volatiles matters. These processes also enable temperature optimization in each reactor for biomass conversion improvement and the production of high heating values gases [8,9].

* Corresponding author at: IMT Mines Albi, UMR CNRS 5302, Centre RAPSODEE, Campus Jarlard, F-81013 Albi Cedex 09, France.
E-mail address: tchini_severin.tanoh@mines-albi.fr (T.S. Tanoh).

Different designs of processes for small-scale plants have been presented in the literature. Small-scale plants are interesting compared to large-scale ones because biomass is dispersed and the negative environmental impact due to its transportation over long distances from various locations can be avoided [10,11]. The small-scale two-stage processes use air to provide energy to the endothermic reactions [1,12,13]. The Belgian company Xylowatt has developed a two-stage gasification process consisting of two fixed bed reactors placed one above the other. The air is injected in the pyrolysis zone to drive oxidative pyrolysis phase and in the tar and gas combustion zone to bring energy to char gasification process. With this process, a syngas with less than 3 g/Nm^3 tar content was produced. However, it contained more than 40 vol% of nitrogen [14]. The Technical University of Denmark (DTU) developed a two-stage gasification process called "Viking" with a nominal thermal input of 75 kW, consisting of a screw reactor for pyrolysis combined with a fixed bed char gasifier. Air is injected for partial oxidation in an intermediate high-temperature tar-cracking zone between the two reactors [15]. Hence, the produced gas contains a very small quantity of tar (<15 mg/Nm^3). However, due to air injection, it is diluted with nitrogen (> 30 vol%) [16]. Although all these processes have proven the feasibility of tar removal from the produced gas, they all produce syngas with high nitrogen content which is a serious issue when it comes to the costs linked to nitrogen/syngas separation.

To reduce the tar formation and also to minimize the syngas dilution, Cortus Energy developed a multistage gasification process called «woodRoll» [17]. It is a three-stage gasification process where the drying and the pyrolysis (350–400 °C) are performed in the two separated rotary kilns, heated indirectly. The gas and the tar from the pyrolysis are fed to a burner where they are combusted with air to heat the whole process. Char is subsequently gasified in the entrained gasifier with steam at 1100 °C. The char gasification with steam produces a syngas nearly free of tar and nitrogen with high H_2 content. However, the real weakness of this process might be the conversion rate inside the gasifier. Indeed, the latter depends strongly on the char reactivity that varies from one biomass to another [18].

The two-stage biomass pyrolysis followed-up by catalytic reforming of volatile matter is largely studied in the literature [19–24]. The catalysts such as nickel-based catalysts, non-nickel metal catalysts (Rh, Ru, Pt, etc), alkali metal catalysts and char are effective in reforming tar and improving the quality of syngas [25]. The catalyst is used in a second reactor and permits to reduce the reforming temperature between 600 °C and 950 °C, to attain complete tar elimination and to increase the yields of H_2 and CO [20,26]. However, the catalysts show some weaknesses such as their rapid deactivation due to certain impurities (sulphur) and high tar content in the volatile matter, and the need for preconditioning of the feed before it enters the catalyst bed [27,28]. In addition, the catalysts are expensive and difficult to recover [27,29].

Our research group is developing a new approach to produce a syngas with a lower amount of nitrogen and tar. This approach consists of using a two-stage pilot-scale gasification process where biomass is pyrolyzed in the first stage, and the volatile matter is cracked and reformed without catalyst in the second one. This approach is robust and can permit to overcome the problems related to the use of catalysts. In a future full-scale process, the pyrolysis char might be combusted to provide the required energy for the whole process. However, this aspect will not be discussed in this paper. In this work, for sake of simplicity, the process is heated electrically.

In this work, we study experimentally the pyrolysis of biomass and non-catalytic reforming of volatile matter. The work aims to validate the feasibility of this suggested process by studying the influence of the operating conditions on its performances. The process consists of two indirectly heated reactors in series: a rotary kiln and a non-catalytic tubular reactor. The rotary kiln is dedicated to the pyrolysis and the tubular reactor to the reforming of the volatile matter which consists of the permanent gases and bio-oil produced during the pyrolysis phase. In this study, bio-oil or liquid refers to the mixture of produced tar and water. All tests were performed at the pilot scale, with green waste and wood as biomass. Wood serves as the biomass of reference.

2. Material and methods

2.1. Biomass characteristics

Two biomass sources were processed. Green waste was supplied by the French company AGRI 2000; wood (a mixture of oak and beech sawdust) was provided by the French company *S.C.A de Deshydration de la Haute-Seine*. The green waste used consists of garden waste which contains mostly small branches, leaf, and grass. However, the quantity of each fraction is not known. To facilitate the flow through the first reactor, green waste was ground and pelletized into uniform cylindrical pellets with a diameter of 6 mm, a length between 6 and 10 mm, and an apparent pellet density of 624 kg/m^3. Wood was already provided as cylindrical pellets also with a diameter of 6 mm, a length between 6 and 15 mm, and an apparent density of 688 kg/m^3. Green waste and wood pellets used in this study were characterized by the methods summarized in Table 1. Analysis results are gathered in Table 2**.** The results show that both biomasses have similar water content. Their chemical compositions are also similar. However green waste is characterized by high ash content. It is richer in silicon and alkali (Ca, K, Mg).

2.2. Two-stages process and experiment procedure

The two-stages pyrolysis-reforming process consists of a rotary kiln where the pyrolysis takes place and a tubular reactor for the reforming of the pyrolysis volatile matter. In this study, both reactors are electrically heated. The thermal control of the two reactors is managed separately. A schematic diagram of the system is shown in Fig. 1.

The rotary kiln is a 4.2 m long cylinder of 0.21 m internal diameter and 2.5 m effective heated length. The reactor is heated by electrical resistances with a power of 38 kW. All experiments were performed with a 3° inclination of the rotary kiln tube, a rotation speed of 3 rpm and a 40 min mean solid residence time. During the experiment, 6 kg/h of biomass were fed into the reactor initially preheated at 800 °C. This temperature has been selected based on pyrolysis experiments carried out previously between 700 °C and 900 °C [31]. It was found that at 700 °C, the residual volatile matter content of the produced char was too high (>10 wt%). On the other hand, it was very low (<5 wt%) at 900 °C. However, to minimize thermal stresses and fatigue undergone by the reactor, the temperature of 800 °C seems to be a good compromise and was retained in the following. When the steady-state was reached (after about 2 h), the gas online analysis and bio-oil sampling are started, simultaneously char is collected in a new container at the reactor outlet. The gas and tar sampling system is shown in Fig. 2. The reproducibility of the pyrolysis experiments has been tested. The mass balance is close to 94% for green waste and 92% for wood.

Volatile matter reforming was carried out in a 1.65 m long tubular reactor with a 75 mm inner diameter. The tubular reactor which consists of three-zones is electrically heated by a total power of 18 kW and can reach 1600 °C along a 1 m isothermal reaction zone. Because of its capacity, only a part of the volatile matter produced in the rotary kiln was transferred to the tubular reactor through a 400 °C heated 10 m long

Table 1
Biomass characteristics and analysis methods.

Biomass characteristics	Methods
Ultimate analysis	Elementary analyzer CHNS-O (FLASH 2000)
Proximate analysis	NFV 03–921 (Moisture), NF MO3–004 (Volatile matter), Ash (NF MO3–004) and Fixed carbon (by difference)
Macromolecular composition	The protocol of Li et al. [30] as well as the standards TAPPI T204 om-88 and TAPPI T22 om-88
Ash composition	EN 16967 (ICP-OES)

Table 2
Properties of the biomass samples.

	Green Waste	Wood
Moisture (wt%)	7.3	7.7
Proximate analysis (wt% dry basis)		
Volatile matter	79.3	82.5
Ash	2.7	0.9
Fixed carbon	18.0	16.6
Ultimate analysis (wt% dry basis)		
C	48.9	49.3
H	5.6	5.9
N	0.3	0.1
O*	42.5	43.8
Macromolecular composition (wt% dry basis)		
Lignin	27.8	26.1
Hemicelluloses	24.0	26.3
Cellulose	39.4	37.6
Extractives	8.8	10.0
Contents in inorganics (mg/kg dry basis)		
Ca	2070	838
K	164	94
Mg	220	46
Fe	392	89
Si	1218	128
Lower heating value (MJ/kg dry basis)		
LHV	17.9	18.1

*O =100-(C+H+N).

line. A pump placed downstream of the tubular reactor was used to circulate the gas. Before reaching the isothermal reaction zone, the volatile matter was preheated at 850 °C using an electrical preheater. The residence time was calculated based on the outgoing volume flow rate, the isothermal reaction zone size, and the temperature. The reforming stage takes place at a temperature of 1200–1300 °C. Two mean residence times were operated around: 5 s and 10 s. The reasons for choosing this temperature range and the residence times are given in section 3.1. To ensure the reliability of the results, the experiment at 1300 °C with a residence time of 10 s was repeated twice. The relative error was less than 5% on the product yields and less than 1% on the gas composition.

2.3. Sampling and analysis

The bio-oil has been sampled by a condensation system consisting of six impinger bottles connected in series. Isopropanol was added in each bottle: 300–400 mL at the exist of the rotary kiln (sampling point 1) and 100 mL at the outlet of the tubular reactor (sampling point 2), except for the fifth one which was left empty and the last one which was filled with silica gel Fig. 2. The gas and bio-oil sampling were performed at a flow rate of 2 L/min using a rotameter. In each experiment, samples of bio-oil were collected in the impinger bottles, for 45 min at the outlet of the rotary kiln and 30 min at the outlet of the tubular reactor. The sampled bio-oil flow rate was determined by weighing the bottles (with isopropanol) before and after sampling. The char was collected at the rotary kiln outlet for 45 min. The soot was collected in three-points: in the

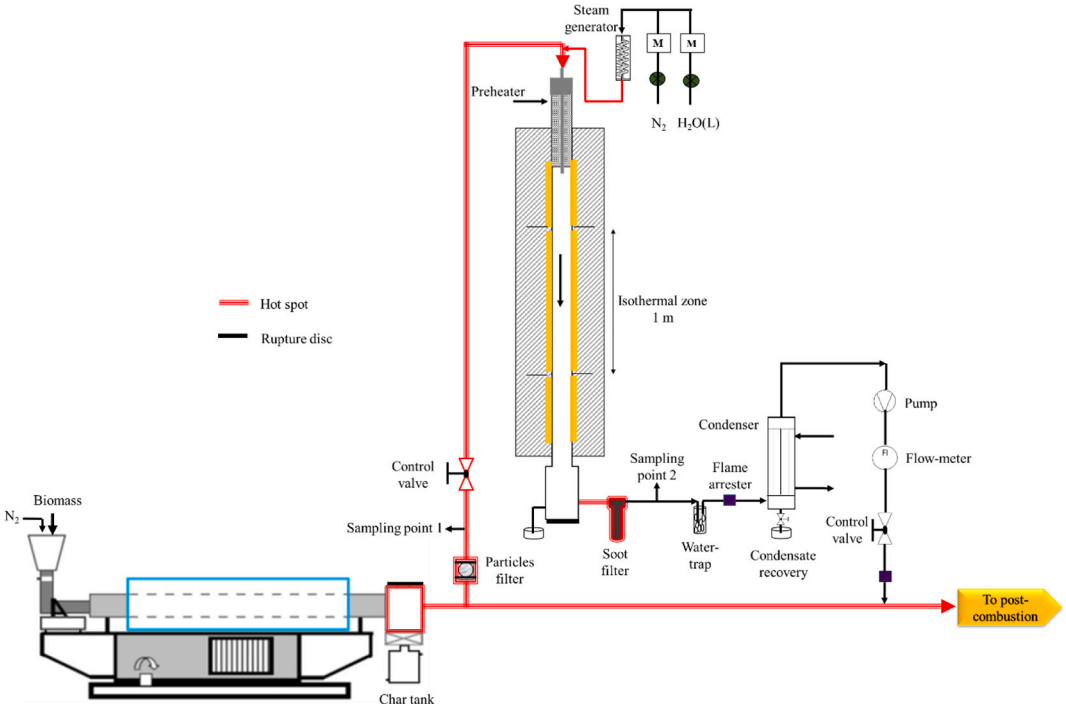

Fig. 1. Experimental setup.

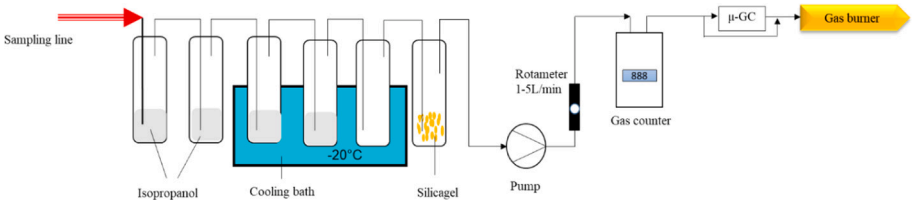

Fig. 2. Gas and bio-oil sampling system.

reactor, the pipeline, and the filter. Soot collection requires the reactor to be cold and free of syngas.

The gas composition including H_2, CO, CH_4, CO_2, C_2H_2, C_2H_4, C_2H_6 and C_3H_8 was analysed by gas chromatography (490 Micro GC, Agilent).

Bio-oil is a mixture of water and tar. Water content in bio-oil was measured by Karl Fisher (METTLER TOLEDO V30) titration using HYDRANAL dry methanol as the solvent and HYDRANAL Composite 5 as the titrant.

Tar analysis was performed using a Shimadzu GC/MS-TQ 8030 (Tokyo/Japan) Gas Chromatograph Mass Spectrometer. Chromatographic separation was performed on a Rxi-5Sil MS (30 m × 0.25 mm, 0.25 μm film thickness, Resteck) column using helium as a carrier gas at a 3.0 mL/min constant flow. The column oven temperature evolution was programmed as follows. First, it was set at an initial value of 40 °C for 5 min. After that 280 °C was reached (with a 5 °C/min rate) and maintained for 2 min. A volume of 1 μL was injected at 250 °C in split mode using 1:10 split ratio. The mass spectrometer operated in the electron impact (EI) ionization mode (electron energy was 70 eV). The interface and ion source temperatures were respectively set at 260 °C and 200 °C. For qualitative analysis, the detection was performed in full scan mode in a 35–600 m/z range. It is important to mention that the tar composition determination is extremely complex given the high number of species to identify. In this study, only the species showing a surface area greater than 2% were taken into consideration. For the quantitative analysis of tar from pyrolysis, the selected ion monitoring (SIM) detection mode was performed with 3 qualifier ions for each component. 10 standard samples (benzene, toluene, m-cresol, m,p-xylene, styrene, naphthalene, fluorene, biphenyl, and phenol) were used for the calibration. These compounds were quantified using calibration curves, which were produced by an analysis of pure substances by GC/MS.

2.4. Mass balance and pilot performance

2.4.1. Pyrolysis mass balance

The nitrogen gas (4 NL/min) was used as a tracer to establish mass balance. The mass flow rate and yield of permanent gases at the reactor outlet were calculated using data from the micro-GC and the mass conservation equation for the tracer gas (N_2) following eqs. 1 and 2 respectively:

$$\dot{m}_{gp} = \frac{\dot{m}_{N_2}}{Y_{N_2}} - \dot{m}_{N_2} \tag{1}$$

$$\eta_{gp} = \frac{\dot{m}_{gp}}{\dot{m}_{biomass\_daf}} \tag{2}$$

where Y_{N2} and $\dot{m}_{N_2}$ are the nitrogen mass fraction in the permanent gases and mass flow rate, respectively. $\dot{m}_{biomass_daf}$is the biomass mass flow rate on a dry ash-free basis. $\eta_{gp}$and $\dot{m}_{gp}$are the permanent gases yield (wt% daf) and mass flow rate, respectively.

The bio-oil mass flow rate and its yield at the outlet of the rotary kiln were determined by Eqs. 3 and 4 respectively:

$$\dot{m}_{bio-oil} = \dot{m}_{gp}\frac{\dot{m}_{bio-oil\_sampled}}{\dot{m}_{gp\_sampled}} \tag{3}$$

$$\eta_{bio-oil} = \frac{\dot{m}_{bio-oil}}{\dot{m}_{biomass\_daf}} \tag{4}$$

where $\dot{m}_{bio-oil\_sampled}$ and $\dot{m}_{gp\_sampled}$ are the mass flow rate of bio-oil and permanent gases sampled by gas and bio-oil sampling system (Fig. 2).

The water content (WK) in bio-oil (wt%.) determined by Karl Fischer allowed calculating the yields of water (η_{water}) and tar (η_{tar}) according to eqs. 5 and 6 respectively:

$$\eta_{water} = \frac{\dot{m}_{bio-oil}\frac{WK}{100} - \dot{m}_0\frac{H_0}{100}}{\dot{m}_{biomass\_daf}} \tag{5}$$

$$\eta_{tar} = \frac{\dot{m}_{bio-oil}\left(1 - \frac{WK}{100}\right)}{\dot{m}_{biomass\_daf}} \tag{6}$$

where $\dot{m}_0$ and H_0 are the initial mass flow rate of biomass (kg/h) and humidity in the biomass (wt%) respectively.

The char was collected and weighted to determine its yield according to eq. 7.

$$\eta_{char} = \frac{\dot{m}_{char}}{\dot{m}_{biomass\_daf}} \tag{7}$$

$\dot{m}_{char}$and $\eta_{char}$are the char mass flow rate and yield (wt% daf) respectively.

2.4.2. Mass balance after cracking and reforming

The syngas outgoing mass flowrate and yield were calculated according to eqs. 8 and 9 respectively:

$$\dot{m}_{syngas} = \rho_{syngas}\dot{V}_{syngas} \tag{8}$$

$$\eta_{syngas} = \frac{\dot{m}_{syngas}}{\dot{m}_{biomass\_daf}} \tag{9}$$

Where $\dot{V}_{syngas}$ and $\rho_{syngas}$are the syngas volume flow rate and mass density, respectively.

The soot from volatile matter reforming was collected and weighted to determine its yield according to Eq. 10.

$$\eta_{soot} = \frac{\dot{m}_{soot}}{\dot{m}_{biomass\_daf}} \tag{10}$$

Bio-oil, tar and water yields were calculated with eqs. 4, 5 and 6 respectively.

2.4.3. Global process performance evaluation

To evaluate global performances of the process, some indicators are used, and calculated by eqs. 11 and 12:

$$Dry\ gas\ yield = \frac{Volume\ flow\ rate\ of\ the\ dry\ product\ gas}{Mass\ flow\ rate\ of\ biomass\ on\ dry\ ash\ free\ basis} \tag{11}$$

$$Cold\ Gas\ Efficiency\ (CGE) = \frac{Chemical\ energy\ in\ the\ reformed\ gas}{Fuel\ input\ energy} \tag{12}$$

3. Results and discussion

This section consists of two parts. The first part is dedicated to biomass pyrolysis at 800 °C and its char and volatile matter yields and composition. The second part is focused on the global process performances.

3.1. Product yield and composition of volatile matter from biomass pyrolysis

Table 3 shows the results for the pyrolysis of green waste and wood at 800 °C. A comparison between the pyrolysis of green waste and wood revealed that slightly higher gas (56 wt%) and lower tar (8 wt%) yields were obtained when the wood is used as raw material. This difference cannot be explained by the organic macromolecules of the two biomass samples because their organic components are similar. Thus, a possible explanation could be the content of mineral components in the two

Table 3
Product yields and gas composition from the pyrolysis of two biomass.

Mass balance (wt% biomass daf basis)		
	Green Waste	Wood
Gas	54.1 ± 0.5	56.0 ± 0.8
Tar	12.7 ± 0.2	8.3 ± 0.3
Water	14.3 ± 0.8	17.8 ± 0.9
Char	18.9 ± 0.5	17.9 ± 0.4
Gas composition (vol%)		
H_2	29.6 ± 1.1	26.1 ± 2.0
CH_4	16.7 ± 1.9	17.3 ± 1.3
CO	31.3 ± 0.4	34.4 ± 1.1
CO_2	18.0 ± 0.5	17.5 ± 0.8
C_2-C_3	4.5 ± 0.1	4.7 ± 0.3

biomass samples [32,33]. The catalytic effect of other inorganic components as alkaline and alkaline earth metals, especially potassium, is demonstrated. However, silicon can melt from 600 °C and then inhibit the catalytic effect of other mineral species [34]. Green waste has a higher content of silicon than wood. This can explain the fact that there is a high content of tar in volatile matters from green waste.

Pyrolysis of the two biomass samples produced similar amounts of char. The char yield does not exceed 20 wt%. In a full-scale process, this char could be used to supply the energy required by the endothermic drying, pyrolysis, and reforming reactions. The process modelling on Aspen Plus V8.6 (not presented in this paper) showed that the combustion of 20% of char with an excess air ratio of 1.13, preheated at 800 °C, gives the flue gas temperature of 1990 °C. If we consider that the initial biomass has 20% of moisture, 20% of char are largely sufficient to make the process autothermal.

The pyrolysis of green waste and wood leads to almost similar gas compositions. However, the gas produced from wood pyrolysis has a slightly higher CO concentration than the one from green waste. On the other hand, the gas produced from green waste pyrolysis is more concentrated in hydrogen. The H_2/CO molar ratios are 0.94 and 0.70 for green waste and wood respectively.

The characterisation of collected tar has been carried out by GC/MS analysis. The qualitative and quantitative analyses were performed to know the composition of tar after pyrolysis in order to fix the operating conditions for cracking and reforming of volatile matter.

Table 4 shows the relative peak area of major chemical components in tar after pyrolysis. Some compounds can be found in both green waste and wood tar. The tar is dominated by light aromatics, which comprise single-ring compounds (benzene, toluene), light and heavy polyaromatic hydrocarbons (PAHs) such as naphtalène, biphenylene or acenaphthylene, fluorene, phenanthrene and fluoranthene. Similar tar composition was observed by Santamaria et al. [35] for wood pellet pyrolysis at 800 °C.

Table 4
Main compounds in tar after pyrolysis identified by GC/MS.

Compounds	Relative content (area %)	
	Green waste	wood
Benzene	34.5	58.1
Toluene	11.6	6.8
p-xylene or o-xylene	0.7	
Styrene		1.6
1,3,5,7-cyclooctatetraene	3.1	
Phenol	1.3	
Benzofuran	1.2	
Benzene, 1-propynyl	6.2	
Indene		4.0
Naphthalene	22.0	25.3
Naphthalene, 2-methyl	2.0	
Naphthalene, 1-methyl	0.9	
Biphenyl	1.0	
Acenaphthylene or biphenylene	4.9	2.1
Dibenzofuran	0.7	
Fluorene	2.1	0.6
Phenanthrene	4.0	1.1
Fluoranthene	1.8	0.4

To get an insight into the quantity of the compounds, quantitative analysis was performed by GC/MS with ten compounds that are generally found after pyrolysis at 800 °C in works from the literature [36,37]. The ten compounds have been given in section 2.3. The tar species yields are presented in Fig. 3. It can be noted that the total mass of compounds quantified by GC/MS is not equal to the sampled tar mass. For wood, the total mass quantified by GC/MS represents 70% of the sampled tar. While for green waste, the total mass quantified by GC/MS represents only 37% of the sampled tar. It can be concluded that the tar from green waste contains a larger variety of species than those of wood. Similar yields of benzene, toluene and naphthalene were obtained in the literature [35,36]. Benzene, toluene, and naphthalene are the major compounds among the quantified tar. It is well-known that toluene, benzene, and naphthalene are stable, hence more difficult to remove [38]. Jess [39] studied the thermal removal of tar (toluene, benzene and naphthalene) in a hydrogen and steam atmosphere. He concluded that temperatures of 1200 °C and residence times less than 10 s are necessary for the thermal conversion of aromatic hydrocarbons in product gases from pyrolysis and gasification of biomass. Materazzi et al. [40] also reported that temperatures above 1000 °C, at reasonable residence times (> 10 s), are necessary to destroy the aromatics, without a catalyst. So, 1200 °C and 1300 °C were selected for the second reactor as well as two residence times: 5 s and 10 s.

3.2. *Global process performances*

To evaluate the global performance of the process, the effect of temperature and residence time on product yields and their composition (mainly gas and tar) is analysed. The results obtained using green waste are compared to those from wood at 1300 °C and with a residence time of 5 s.

3.2.1. *Effect of reforming temperature on the global process mass balance*

The influence of the non-catalytic reforming temperature on the product yields is presented in Fig. 4. Tar concentration in the syngas is also given in Table 5. Tar yield decreases from 12.7 wt% (224 g/Nm3) after pyrolysis at 800 °C down to 5.6 wt% (71.6 g/Nm3) at 1200 °C with 5 s; this represents a conversion rate of 56%. Tar yield also decreases from 12.7 wt% after pyrolysis at 800 °C down to 2.6 wt% (30.7 g/Nm3) at 1300 °C with 5 s; this represents a conversion rate of 80.4%. The conversion rate of tar increases with the increasing temperature, but it

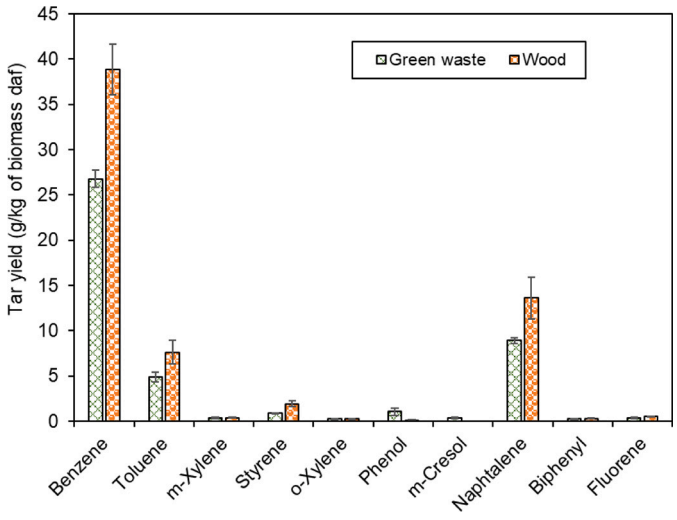

Fig. 3. Tar species yields from the biomass pyrolysis.

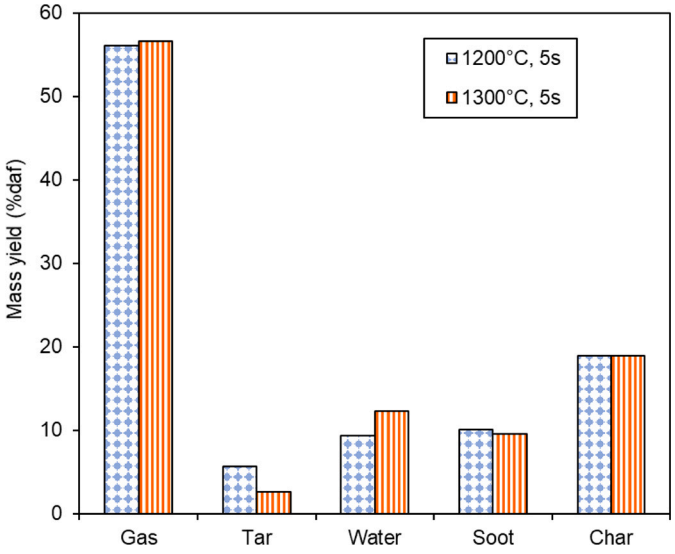

Fig. 4. Mass balance for green waste after reforming at 1200 °C and 1300 °C, with a gas residence time of 5 s.

Table 5
Process performance and syngas quality.

	Green waste, 1200 °C, 5 s	Green waste, 1300 °C, 5 s	Green waste, 1300 °C, 10s	Wood, 1300 °C, 5 s
Tar concentration (g/Nm^3)	71.6	30.7	0.15 ± 0.04	1.3
Lower heating value of syngas (MJ/Nm^3)	11.4	11.1	11.06 ± 0.02	11.05
Cold Gas Efficiency (%)	48.7	50.9	47.42 ± 1.45	48.95
Dry gas yield (Nm^3/kg daf)	0.78	0.85	0.79 ± 0.03	0.81

remains relatively high tar content in syngas. This means that the tar produced after pyrolysis is very refractory and hard to crack under these operating conditions.

It was expected that thermal cracking results in the conversion of tar into light gases. However, this effect was not substantial, and the observed gas yields were 56.1 wt% at 1200 °C and 56.6 wt% at 1300 °C. It represents an increase of only 3.7%. Gas yield after cracking and reforming is not significantly impacted by the operating conditions. Almost all tar is converted into soot. The soot yield is 10.1 wt% at 1200 °C and 9.6% at 1300 °C. The slight decrease of soot yield at 1300 °C may be explained by steam and CO_2 gasification of soot following reaction (R1) and reaction (R2) (Boudouard reaction) respectively, which could explain the decrease of CO_2, as well as the increase of H_2 and CO as mentioned in section 3.2.2 [40,41]. The soot formation should not be a surprise. Indeed, it is reported in the literature that tar thermal cracking can produce soot at high temperatures (1000–2500 °C) [40,42]. Under the condition of high temperature, PAHs play the role of precursor and undergo processes of polymerization, condensation and growing into soot particles [43]. Soot is mostly carbon; other elements such as hydrogen and oxygen are usually present in small amount. The important quantity of soot formed will impact the overall efficiency of this process. For instance, 10% of formed soot with a typical LHV of 30 MJ/kg represents 17% of the initial wood LHV. Soot will also create technical challenges in processes, e.g. clogging of flow passages and fouling on system components [44].

it is observed that tar cracking is also accompanied by water formation. In this work, the water yield increases from 9.3 wt% at 1200 °C to 12.3 wt% at 1300 °C. According to the literature, the formation of water and the increase of its yield with temperature can be considered as an indicator of the extent of heavy hydrocarbons cracking reactions [45,46].

$$C(s) + H_2O \rightarrow CO + H_2 \quad \text{(R1)}$$

$$C(s) + CO_2 \rightarrow 2CO \quad \text{(R2)}$$

3.2.2. *Effect of reforming temperature on the syngas composition*

The influence of the non-catalytic reforming temperature on the syngas composition is displayed in Fig. 5. The content of H_2 in syngas increases remarkably from 29 vol% after pyrolysis to 50 vol% at 1200 °C and 53.5% at 1300 °C. Also, the CO content increase slightly. This may be attributed to alkyl aromatization reaction which is promoted at these temperatures, steam reforming of tar, and water-gas reaction [47].

Table 5 gives the results of cold gas efficiency (CGE) of the process and the lower heating values (LHV) of the syngas. They are important parameters to appreciate syngas quality and process performance. The obtained syngas is of very good quality regarding their LHV. The cold gas efficiency increases slightly from 48.7% at 1200 °C to 50.9% at 1300 °C. It can be considered low compared to [48], which is a consequence of a large amount of remaining tar, soot and char formed. CO_2, CH_4 and C_2-C_3 concentrations decrease significantly when the temperature is increased. The decrease in CO_2 concentration could be due to its reaction with hydrocarbons (dry reforming) or soot to form CO (Boudouard reaction). According to the literature, these reactions are favoured by high temperatures and lead to hydrocarbons concentration decrease, and H_2 and CO concentration increase [49]. Besides, the formed soot could be gasified by CO_2, which causes the reduction of the CO_2. According to Qin et al. [42], a higher temperature (>1200 °C) reverses the exothermic water gas shift reaction, which can also reduce the CO_2 concentration. CH_4 concentration strongly decreases at a higher temperature. This might be due to dry and steam reforming reactions but also to its potential degradation to form soot.

In this work, the H_2/CO_2 ratio is higher than 7 and the H_2/CO ratio is 1.4 and remains unchanged at 1200 °C and 1300 °C. According to this, the produced syngas can be used in several applications, including biological methanation. The biological methanation pathway is particularly interesting because it avoids the use of vulnerable and expensive catalysts, no need for syngas reheating between 300 and 400 °C, lower requirement for syngas cleaning, etc. in comparison to catalytic methanation [50]. It is worth noting that some authors recommend the H_2/CO and H_2/CO_2 ratios of 3 and 4 respectively to obtain the full

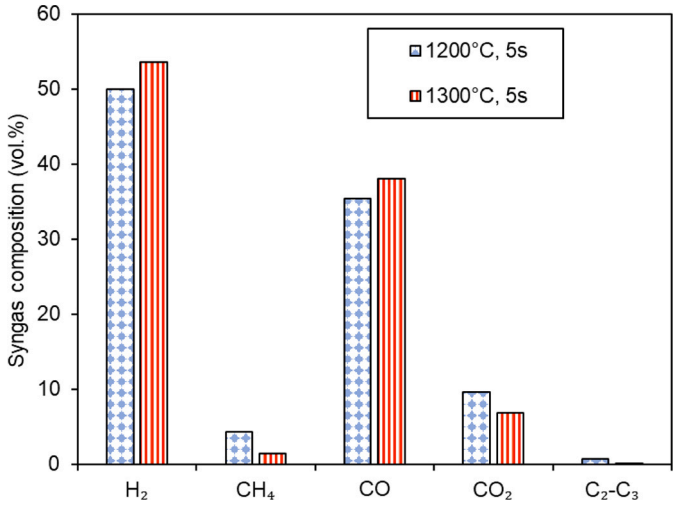

Fig. 5. Syngas composition from green waste after reforming at 1200 °C and 1300 °C, with a gas residence time of 5 s.

conversion of all CO and CO_2 towards CH_4. However, it has been proven that higher H_2/CO_2 ratios could be used depending on the operating conditions (temperature, bioreactors, etc.) and micro-organisms [51].

It can be concluded that the cracking and reforming of pyrolysis volatile matter at 1200 °C and 1300 °C with a gas residence of 5 s impact very slightly the gas yield and leads to the formation of soot. The results suggest that it is difficult to remove tar for green waste in the studied operating conditions.

3.2.3. *Effect of residence time on global process mass balance and syngas composition*

The effect of residence time on product yields and syngas composition is shown in Fig. 6 and Fig. 7. The longer residence time was achieved by decreasing the gas flow at the inlet of the reforming reactor. The soot yield increases from 9.6 to 11.5 wt% when the gas residence time increases from 5 to 10 s, while the tar yield decreases strongly from 2.5 to 0.01 wt%. The tar reduction is dramatically affected by the residence time. On the other hand, polycyclic aromatic hydrocarbons (PAHs) formation such as naphthalene, phenanthrene, fluorene, etc. is also observed. It was demonstrated that the PAHs are precursors of soot and the latter one is specifically the result of reactions between PAHs [44]. Thus, one can conclude that a long residence time provided conditions for the growth of PAHs and the reactions between them to form more soot. The increasing gas residence also leads to a decrease in the syngas yield from 56.6 to 52.3 wt%. A similar trend was observed by [52]. Probably, the latter can be converted into water by water gas shift reaction and into tar. Furthermore, an increase in water yield can be observed. Also, since the cold gas efficiency is related to the syngas yield and composition, it decreases by 7% (Table 5). The individual gas concentrations are almost kept constant. Increasing residence time does not affect the gas composition. H_2/CO ratio remains constant at 1.4.

The increasing gas residence time at 1300 °C has increased the yield of soot and decreased drastically the amount of tar and syngas yield. The tar concentration in the syngas is 0.15 g/Nm^3.

3.2.4. *Tar composition at reforming output*

The research works conducted by Trabold et al. [7] revealed that some compounds of tar impacted negatively the biological methanation of gasification syngas. Therefore, it appears essential to analyse qualitatively and quantitatively the produced tar. But only qualitative analysis of tar is presented.

Table 6 shows the qualitative analysis of the produced tar at the cracking and reforming output at different temperature and gas residence time. The reforming stage tar consists of 1-ring aromatic hydrocarbons, 2-ring and 3–6 rings PAH compounds. The results show that the reforming temperature and residence time play an important role in the changing composition of tar. At 1200 °C, 1-ring compounds, and PAHs with 2–6 rings are found in the tar composition, whereas with increasing the reforming temperature to 1300 °C and residence time, only PAHs with 2–3 rings are dominant. The disappearance of 1-ring aromatic hydrocarbons with the increase of the reforming temperature and residence time could be attributed to their combination reactions [53]. For instance, Zhang et al. [54] reported that biphenyl is formed by a combination of two phenyl rings. These compounds are generated by the release of the H^+ radicals from the benzene. Benzo[*ghi*]perylene, pyrene and fluoranthene (heavy PAHs) are only detected at 1200 °C. This may seem contradictory because it is well known that when the temperature increases, PAHs grow. However, two phenomena might be at the origin of such results. According to Nguyen et al. [55], the growth of PAHs can be eliminated when the severity of the process is sufficient to convert the steam and H_2 into the reactive hydrogen intermediates that prevent the combination of carbon-containing species to form the heavier compounds.

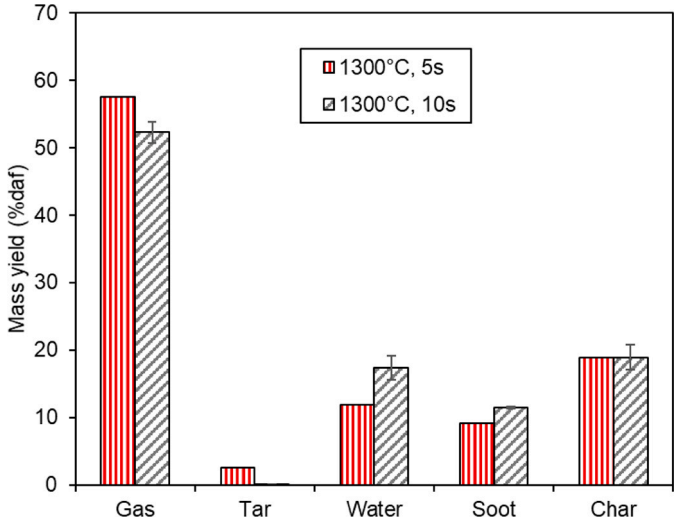

Fig. 6. Mass balance for green waste after reforming at 1300 °C, with the gas residence time of 5 s and 10 s.

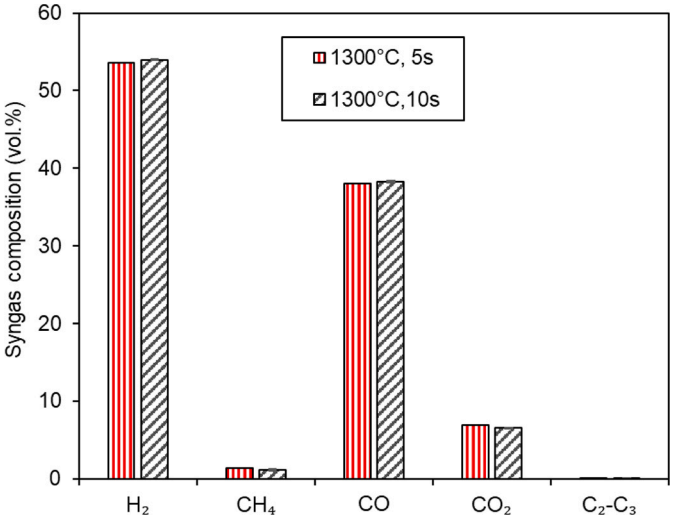

Fig. 7. Syngas composition from green waste after reforming at 1300 °C, with the gas residence time of 5 s and 10 s.

3.3. *Comparison between reforming products of green waste and wood*

In this section, the results of green waste volatile matter reforming at the most favourable temperature of tar reduction (1300 °C) are compared to those of the biomass of reference (wood). The mass balance of wood products and gas composition at 1300 °C with the gas residence time of 5 s is presented in Fig. 8 and Fig. 9 respectively, and compared to that of green waste. The results show that under the same conditions, the tar conversion ratio is 98.8% for wood and 80.4% for green waste. A similar result was observed by Chen and al. [56]. This can be explained by the fact that wood tar has a different composition than tar from green waste. As it was mentioned in section 3.1, the GC/MS quantification of the wood tar has allowed quantifying 70% of sampled tar, which is essentially dominated by benzene, toluene, and naphthalene. Thus, the tar conversion ratio obtained for wood is in agreement with the literature which suggests complete elimination of the toluene at 1000 °C, and of benzene and naphthalene at 1300 °C [38].

The soot yield for wood is slightly lower. This is because wood produces less tar after pyrolysis. Trubetskaya et al. [57] found similar yields of soot for two types of wood (pine and beech) between 1250 °C and 1400 °C.

The syngas composition is comparable. The slight difference

Table 6
Main compounds in tar after cracking and reforming identified by GC/MS.

	Green waste,1200 °C, 5 s	Green waste,1300 °C, 5 s	Green waste,1300 °C, 10s	Wood, 1300 °C, 5 s
Benzene	32.8			
o-Xylene	28.3			
Naphthalene	12.3	62.8	28.4	42.5
Naphthalene, 2-methyl-		6.3	3.2	
Biphenyl		4.8		
Naphthalene, 2-ethenyl-			2.2	
Acenaphthylene	6.9	26.0	34.5	
Biphenylene				25.1
Dibenzofuran			3.6	
Fluorene	2.2		15.4	5.3
Phenanthrene	4.5		12.8	22.7
Pyrene	2.1			4.4
Fluoranthene	2.2			
Benzo[*ghi*]perylene	8.7			

Fig. 8. Mass yield for green waste and wood after reforming at 1300 °C and a gas residence time of 5 s.

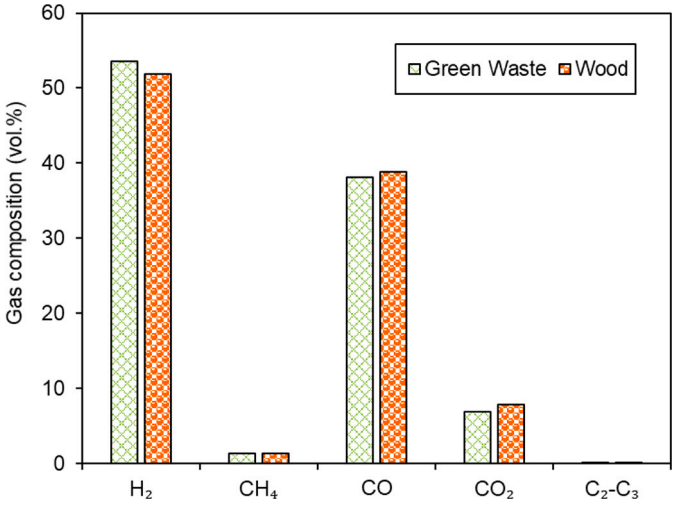

Fig. 9. Composition of syngas from green waste and wood after reforming at 1300 °C and a gas residence time of 5 s.

observed with cold gas efficiency is mainly because green waste produces more syngas than wood.

Table 6 shows that the tar composition from the two biomasses presents some differences. The tar from wood contains the 2–3 ring PAHs, while there are no 3-ring components in the tar from green waste at the same conditions.

4. Conclusion

A two-stage pilot-scale process has been developed at centre RAPSODEE of IMT Mines-Albi. Experiments have been performed to validate the feasibility to produce a nitrogen-free syngas by coupling a rotary kiln and a tubular reactor. Green waste and wood, which mainly differ in their ash content, have been used as feedstocks.

The pyrolysis in the rotary kiln at 800 °C has given about 20% of char which can be used to provide the heat to the process. The conversion efficiency of the volatile matter into syngas has been evaluated at different operating conditions in the tubular reactor.

The results have shown that at the two cracking and reforming operating temperatures of 1200 °C and 1300 °C, with a gas residence of 5 s, the formed tar in the pyrolysis stage is mainly converted into soot. The tar conversion ratio is high at 98.8% for wood at 1300 °C, with a gas residence of 5 s. However, for green waste, at the same operating conditions, the tar conversion ratio is 80.4% only. This is probably due to the composition of tar. For the two feedstocks, the syngas yield is not significantly impacted by the increase in temperature. The syngas is rich in H_2 (53 vol%) and CO (38 vol%) and contains CO_2 and CH_4. Its lower heating value is around 11 MJ/Nm^3 and the cold gas efficiency of the process reaches 51%.

Multiplying by two the gas residence time at 1300 °C permits to reduce green waste tar after pyrolysis by 99.9%. But a large part of tar is converted into soot with a yield of up to 11.5 wt% of the initial biomass. The syngas yield also decreases from 56.6% down to 52.3%.

The syngas can be used for producing biomethane via the biological methanation process. This study provides information about the composition of tar remaining after cracking and reforming. Their impact on the microorganisms can be evaluated.

The significant quantities of produced soot may be a limitation for developing this process at a larger scale. The upcoming work will be focused on reducing soot formation.

Author statement

We certify that this manuscript has not been published and is not under consideration for publication by any other journal. All the authors declare that there are no conflicts of interest.

Declaration of Competing Interest

The authors declare that they have no known competing financial interests or personal relationships that could have appeared to influence the work reported in this paper.

Acknowledgements

The authors gratefully acknowledge the financial support from ADEME (1703C0064) and Occitanie Region (ESR_R&F_DF-000043/2017-006713) and express their gratitude to Mrs. Louise Roques, Mr. Maxime Rojas, Mr. Mickael Ribeiro, Mr. Pierre Bertorelle and Mr. Denis Marty for their assistance and contribution to experimental device design and operation.

References

[1] H. Pei, X. Wang, X. Dai, B. Jin, Y. Huang, A novel two-stage biomass gasification concept: Design and operation of a 1.5 MWth demonstration plant, Bioresour. Technol. (2018), https://doi.org/10.1016/j.biortech.2018.07.021.

[2] C.A. Salman, S. Schwede, E. Thorin, J. Yan, Enhancing biomethane production by integrating pyrolysis and anaerobic digestion processes, Appl. Energy 204 (2017) 1074–1083, https://doi.org/10.1016/j.apenergy.2017.05.006.

[3] R. Chandra, H. Takeuchi, T. Hasegawa, Methane production from lignocellulosic agricultural crop wastes: A review in context to second generation of biofuel production, Renew. Sust. Energ. Rev. (2012), https://doi.org/10.1016/j.rser.2011.11.035.

[4] M. Niu, Y. Huang, B. Jin, S. Liang, Q. Dong, H. Gu, R. Sun, A novel two-stage enriched air biomass gasification for producing low-tar high heating value fuel gas: Pilot verification and performance analysis, Energy (2019), https://doi.org/10.1016/j.energy.2019.02.068.

[5] G. Calì, P. Deiana, C. Bassano, S. Meloni, E. Maggio, M. Mascia, A. Pettinau, Syngas production, clean-up and wastewater management in a demo-scale fixed-bed updraft biomass gasification unit, Energies (2020), https://doi.org/10.3390/en13102594.

[6] R. Rauch, J. Hrbek, H. Hofbauer, Biomass gasification for synthesis gas production and applications of the syngas, Adv. Bioenergy Sustain. Chall. (2015) 73–91, https://doi.org/10.1002/9781118957844.ch7.

[7] T. Trabold, M. Neubert, M. Dillig, J. Karl, in: Direct Biological Methanation of the Synthesis Gas of an Allothermal Wood Gasifier, 26th Eur. BIOMASS Conf, 2018.

[8] P. Brandt, E. Larsen, U. Henriksen, High Tar Reduction in a Two-Stage Gasifier, Energy Fuel 14 (2000) 816–819, https://doi.org/10.1021/ef990182m.

[9] T. Bui, R. Loof, S.C. Bhattacharya, Multi-stage reactor for thermal gasification of wood, Energy. 19 (1994) 397–404, https://doi.org/10.1016/0360-5442(94)90118-X.

[10] A. Tremel, M. Gaderer, H. Spliethoff, Small-scale production of synthetic natural gas by allothermal biomass gasification, Int. J. Energy Res. 37 (2013) 1318–1330, https://doi.org/10.1002/er.2933.

[11] C.A. Díaz González, L. Pacheco Sandoval, Sustainability aspects of biomass gasification systems for small power generation, Renew. Sust. Energ. Rev. 134 (2020) 110180, https://doi.org/10.1016/j.rser.2020.110180.

[12] D.R. Nhuchhen, P.A. Salam, Experimental study on two-stage air supply downdraft gasifier and dual fuel engine system, Biomass Convers. Biorefinery. 2 (2012) 159–168, https://doi.org/10.1007/s13399-012-0041-7.

[13] L.I. Chaves, M.J. Da Silva, S.N.M. De Souza, D. Secco, H.A. Rosa, C.E.C. Nogueira, E.P. Frigo, Small-scale power generation analysis: Downdraft gasifier coupled to engine generator set, Renew. Sust. Energ. Rev. 58 (2016) 491–498, https://doi.org/10.1016/j.rser.2015.12.033.

[14] Y. Richardson, M. Drobek, A. Julbe, J. Blin, F. Pinta, Biomass Gasification to Produce Syngas, 2015, https://doi.org/10.1016/B978-0-444-63289-0.00008-9.

[15] J. Ahrenfeldt, U. Henriksen, T.K. Jensen, B. Gøbel, L. Wiese, A. Kather, H. Egsgaard, Validation of a Continuous combined Heat and Power (CHP) operation of a Two-Stage Biomass Gasifier, Energy Fuel 20 (2006) 2672–2680, https://doi.org/10.1021/ef0503616.

[16] U. Henriksen, J. Ahrenfeldt, T.K. Jensen, B. Gøbel, J.D. Bentzen, C. Hindsgaul, L. H. Sørensen, The design, construction and operation of a 75kW two-stage gasifier, Energy. 31 (2006) 1542–1553, https://doi.org/10.1016/j.energy.2005.05.031.

[17] A. Phounglamcheik, M.U. Babler, P. Donaj, M. Amovic, R. Ljunggren, K. Engvall, Pyrolysis of Wood in a Rotary Kiln Pyrolyzer: Modeling and pilot Plant Trials, Energy Procedia 105 (2017) 908–913, https://doi.org/10.1016/j.egypro.2017.03.413.

[18] L.M. Romero Millán, F.E. Sierra Vargas, A. Nzihou, Steam gasification behavior of tropical agrowaste: A new modeling approach based on the inorganic composition, Fuel (2019), https://doi.org/10.1016/j.fuel.2018.07.053.

[19] A. Arregi, G. Lopez, M. Amutio, I. Barbarias, L. Santamaria, J. Bilbao, M. Olazar, Regenerability of a Ni catalyst in the catalytic steam reforming of biomass pyrolysis volatiles, J. Ind. Eng. Chem. (2018), https://doi.org/10.1016/j.jiec.2018.07.030.

[20] A. Arregi, M. Amutio, G. Lopez, J. Bilbao, M. Olazar, Evaluation of thermochemical routes for hydrogen production from biomass: a review, Energy Convers. Manag. 165 (2018) 696–719, https://doi.org/10.1016/j.enconman.2018.03.089.

[21] A.S. Al-Rahbi, J.A. Onwudili, P.T. Williams, Thermal decomposition and gasification of biomass pyrolysis gases using a hot bed of waste derived pyrolysis char, Bioresour. Technol. 204 (2016) 71–79, https://doi.org/10.1016/j.biortech.2015.12.016.

[22] L. Santamaria, G. Lopez, A. Arregi, M. Artetxe, M. Amutio, J. Bilbao, M. Olazar, Catalytic steam reforming of biomass fast pyrolysis volatiles over Ni–Co bimetallic catalysts, J. Ind. Eng. Chem. 91 (2020) 167–181, https://doi.org/10.1016/j.jiec.2020.07.050.

[23] H.D. Setiabudi, M.A.A. Aziz, S. Abdullah, L.P. Teh, R. Jusoh, Hydrogen production from catalytic steam reforming of biomass pyrolysis oil or bio-oil derivatives: a review, Int. J. Hydrog. Energy 45 (2020) 18376–18397, https://doi.org/10.1016/j.ijhydene.2019.10.141.

[24] Q.M.K. Waheed, P.T. Williams, Hydrogen Production from High Temperature Pyrolysis/Steam Reforming of Waste Biomass: Rice Husk, Sugar Cane Bagasse, and Wheat Straw, Energy Fuel 27 (2013) 6695–6704, https://doi.org/10.1021/ef401145w.

[25] N. Wang, D. Chen, U. Arena, P. He, Hot char-catalytic reforming of volatiles from MSW pyrolysis, Appl. Energy 191 (2017) 111–124, https://doi.org/10.1016/j.apenergy.2017.01.051.

[26] A. Arregi, M. Amutio, G. Lopez, M. Artetxe, J. Alvarez, J. Bilbao, M. Olazar, Hydrogen-rich gas production by continuous pyrolysis and in-line catalytic reforming of pine wood waste and HDPE mixtures, Energy Convers. Manag. 136 (2017) 192–201, https://doi.org/10.1016/j.enconman.2017.01.008.

[27] S. Anis, Z.A. Zainal, Tar reduction in biomass producer gas via mechanical, catalytic and thermal methods: A review, Renew. Sust. Energ. Rev. 15 (2011) 2355–2377, https://doi.org/10.1016/j.rser.2011.02.018.

[28] R.A. Arnold, J.M. Hill, Catalysts for gasification: a review, Sustain. Energy Fuels. 3 (2019) 656–672, https://doi.org/10.1039/c8se00614h.

[29] M.D. Argyle, C.H. Bartholomew, Heterogeneous catalyst deactivation and regeneration: a review, Catalysts. 5 (2015) 145–269, https://doi.org/10.3390/catal5010145.

[30] S. Li, S. Xu, S. Liu, C. Yang, Q. Lu, Fast pyrolysis of biomass in free-fall reactor for hydrogen-rich gas, Fuel Process. Technol. 85 (2004) 1201–1211, https://doi.org/10.1016/j.fuproc.2003.11.043.

[31] T.S. Tanoh, A. Ait Oumeziane, J. Lemonon, F.J. Escudero Sanz, S. Salvador, Green Waste/Wood Pellet Pyrolysis in a Pilot-Scale Rotary Kiln: effect of Temperature on product distribution and Characteristics, Energy Fuel 34 (2020) 3336–3345, https://doi.org/10.1021/acs.energyfuels.9b04365.

[32] V. Gargiulo, P. Giudicianni, M. Alfè, R. Ragucci, Influence of possible interactions between biomass organic components and alkali metal ions on steam assisted pyrolysis: a case study on Arundo donax, J. Anal. Appl. Pyrolysis 112 (2015) 244–252, https://doi.org/10.1016/j.jaap.2015.01.018.

[33] L.M. Romero Millán, F.E. Sierra Vargas, A. Nzihou, Unraveled mechanisms in energy production from bioresources using steam gasification, Fuel. 287 (2021) 119527, https://doi.org/10.1016/j.fuel.2020.119527.

[34] M.E. Boot-Handford, E. Virmond, N.H. Florin, R. Kandiyoti, P.S. Fennell, Simple pyrolysis experiments for the preliminary assessment of biomass feedstocks and low-cost tar cracking catalysts for downdraft gasification applications, Biomass Bioenergy 108 (2018) 398–414, https://doi.org/10.1016/j.biombioe.2017.10.048.

[35] L. Santamaria, M. Beirow, F. Mangold, G. Lopez, M. Olazar, M. Schmid, Z. Li, G. Scheffknecht, Influence of temperature on products from fluidized bed pyrolysis of wood and solid recovered fuel, Fuel. 283 (2021) 118922, https://doi.org/10.1016/j.fuel.2020.118922.

[36] A. Dufour, E. Masson, P. Girods, Y. Rogaume, A. Zoulalian, Evolution of aromatic tar composition in relation to methane and ethylene from biomass pyrolysis-gasification, Energy Fuel 25 (2011) 4182–4189, https://doi.org/10.1021/ef200846g.

[37] M.M. Win, M. Asari, R. Hayakawa, H. Hosoda, J. Yano, S.-I. Sakai, Gas and tar generation behavior during flash pyrolysis of wood pellet and plastic, J. Mater. Cycles Waste Manag. 22 (2020) 547–555, https://doi.org/10.1007/s10163-019-00949-8.

[38] R. Maiti, S. Ghosh, S. De, Cracking of tar by steam reforming and hydrogenation: an equilibrium model development, Biomass Convers. Biorefinery. 3 (2013) 103–111, https://doi.org/10.1007/s13399-012-0065-z.

[39] A. Jess, Mechanisms and kinetics of thermal reactions of aromatic hydrocarbons from Pyrolysis of Solid Fuels, Fuel. 75 (1996) 1441–1448.

[40] M. Materazzi, P. Lettieri, L. Mazzei, R. Taylor, C. Chapman, Tar evolution in a two stage fluid bed-plasma gasification process for waste valorization, Fuel Process. Technol. (2014), https://doi.org/10.1016/j.fuproc.2014.06.028.

[41] Y. Chhiti, M. Peyrot, S. Salvador, Soot formation and oxidation during bio-oil gasification: experiments and modeling, J. Energy Chem. 22 (2013) 701–709, https://doi.org/10.1016/S2095-4956(13)60093-5.

[42] K. Qin, W. Lin, P.A. Jensen, A.D. Jensen, High-temperature entrained flow gasification of biomass, Fuel. 93 (2012) 589–600, https://doi.org/10.1016/j.fuel.2011.10.063.

[43] X. Wang, S. Bai, Q. Jin, S. Li, Y. Li, Y. Li, H. Tan, Soot formation during biomass pyrolysis: effects of temperature, water-leaching, and gas-phase residence time, J. Anal. Appl. Pyrolysis (2018) 0–1. doi:https://doi.org/10.1016/j.jaap.2018.07.015.

[44] B. Göktepe, K. Umeki, R. Gebart, Does distance among biomass particles affect soot formation in an entrained flow gasification process? Fuel Process. Technol. 141 (2016) 99–105, https://doi.org/10.1016/j.fuproc.2015.06.038.

[45] C. Di Blasi, Modeling chemical and physical processes of wood and biomass pyrolysis, Prog. Energy Combust. Sci. 34 (2008) 47–90, https://doi.org/10.1016/j.pecs.2006.12.001.

[46] C. Di Blasi, Combustion and gasification rates of lignocellulosic chars, Prog. Energy Combust. Sci. (2009), https://doi.org/10.1016/j.pecs.2008.08.001.

[47] A. Veses, O. Sanahuja-Parejo, I. Martínez, M.S. Callén, J.M. López, T. García, R. Murillo, A pyrolysis process coupled to a catalytic cracking stage: a potential waste-to-energy solution for mattress foam waste, Waste Manag. 120 (2021) 415–423, https://doi.org/10.1016/j.wasman.2020.09.052.

[48] A. Soria-Verdugo, L. Von Berg, D. Serrano, C. Hochenauer, R. Scharler, A. Anca-Couce, Effect of bed material density on the performance of steam gasification of biomass in bubbling fluidized beds, Fuel. 257 (2019) 116118, https://doi.org/10.1016/j.fuel.2019.116118.

[49] S.N. Kriengsak, R. Buczynski, J. Gmurczyk, A.K. Gupta, Hydrogen production by high-temperature steam gasification of biomass and coal, Environ. Eng. Sci. 26 (2009) 739–744, https://doi.org/10.1089/ees.2008.0246.
[50] Antonio Grimalt-Alemany, Ioannis V. Skiadas, Hariklia N. Gavala, Syngas biomethanation: state-of-the-art review and perspectives, Biofuels Bioprod. Biorefin. (2017), https://doi.org/10.1002/bbb.
[51] H. Alwin, V.K. Han, Transportation Biofuels Novel Pathwats for the Production of Ethanol, Biogas and Biodiesel, 2009, https://doi.org/10.1039/9781849732277.
[52] W.R. Hesp, P.L. Waters, Thermal cracking of Tars and Volatile Matter from Coal Carbonization, Ind. Eng. Chem. Prod. Res. Dev. 9 (1970) 194–202, https://doi.org/10.1021/i360034a016.
[53] M. Cortazar, J. Alvarez, G. Lopez, M. Amutio, L. Santamaria, J. Bilbao, M. Olazar, Role of temperature on gasification performance and tar composition in a fountain enhanced conical spouted bed reactor, Energy Convers. Manag. 171 (2018) 1589–1597, https://doi.org/10.1016/j.enconman.2018.06.071.
[54] Z. Zhang, S. Pang, Experimental investigation of tar formation and producer gas composition in biomass steam gasification in a 100 kW dual fluidised bed gasifier, Renew. Energy (2019), https://doi.org/10.1016/j.renene.2018.07.144.
[55] H.N.T. Nguyen, M. Seemann, H. Thunman, Fate of polycyclic aromatic hydrocarbons during tertiary tar formation in steam gasification of biomass, Energy Fuel 32 (2018) 3499–3509, https://doi.org/10.1021/acs.energyfuels.7b03558.
[56] Y. Chen, Y.H. Luo, W.G. Wu, Y. Su, Experimental investigation on tar formation and destruction in a lab-scale two-stage reactor, Energy Fuel 23 (2009) 4659–4667, https://doi.org/10.1021/ef900623n.
[57] A. Trubetskaya, P.A. Jensen, A.D. Jensen, A.D. Garcia Llamas, K. Umeki, D. Gardini, J. Kling, R.B. Bates, P. Glarborg, Effects of several types of biomass fuels on the yield, nanostructure and reactivity of soot from fast pyrolysis at high temperatures, Appl. Energy 171 (2016) 468–482, https://doi.org/10.1016/j.apenergy.2016.02.127.